3D Chemical Scaffolds

DOI: 10.1002/anie.201007107

Three-Dimensional Chemical Patterns for Cellular Self-Organization**

*Yevgeniy V. Kalinin, Jatinder S. Randhawa, and David H. Gracias**

In nature, three-dimensional (3D) chemical patterns are generated and sustained with precisely controlled spatial and temporal profiles on a variety of length and time scales.[1,2] Several studies have outlined the need for the development of in vitro methodologies that replicate the 3D spatiotemporal chemical patterns associated with chemotaxis, cell signaling, angiogenesis, homeostasis, and immune surveillance.[3–7] There are a number of in vitro microfluidic systems that have been developed to mimic in vivo chemical microenvironments, such as the creation of interleukin-8 gradients to study neutrophil chemotaxis.[8] However, microfluidic systems are inherently planar (2D), and their overall size and dependency on external equipment to enable active flow restricts their applicability.[9–11] Hence, the development of passive systems that enable the diffusion-based formation of 3D chemical patterns is attractive, since these systems can be readily utilized to generate and sustain patterns within cell culture, homogeneous gels, and other stationary media. Existing microparticles and reservoirs[12] can be utilized to create chemical patterns in 3D environments; however, the predominant spatial release profile is spherically symmetric[13] (Figure 1 a).

Herein, we argue that 3D spatiotemporal patterns can be created when chemicals are allowed to diffuse out from precisely shaped and patterned hollow containers placed in stationary media. For example, one can vary the shape and symmetry of the overall container as well as the wall porosity pattern to generate a large number of symmetrical and asymmetrical chemical-release profiles. Conceptually, in stationary media, chemical patterns can be generated from spherical or cylindrical geometries by engineering the release rate through control of the wall-porosity characteristics (Figure 1 a–c). However, it is challenging to fabricate spherical or cylindrical containers with precisely patterned sidewalls (such as that shown in Figure 1 c). Alternatively, these geometries can be approximated by polyhedral containers with precisely patterned sidewalls. Hollow polyhedral containers (Figure 1 d–f) can be constructed by the self-folding[14–17] of patterned 2D panels (Figure 1 g–i).

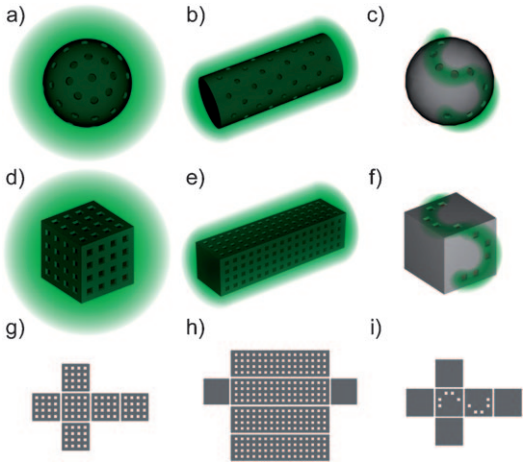

Figure 1. Proposed approach to the generation of 3D chemical patterns: a,b) Schematic diagrams of conceptual spherical or cylindrical containers with uniform wall porosity. c) Further control over the shape and duration of the chemical distribution is afforded by selective patterning of pores on the surface of the container. d–f) Schematic diagrams of our proposed polyhedral containers, which can be designed with a variety of shapes and sizes that approximate, for example, spherical or cylindrical containers. g–i) Precisely patterned 2D panels that can self-fold through surface tension forces into the desired polyhedral containers; numerical simulations guide pore design.

To generate a specific 3D chemical pattern, we first design a polyhedron with approximately the same size and symmetry as the desired pattern. Numerical simulations modeling the diffusion of the specific chemical release from this polyhedron are carried out with different pore sizes and patterns to determine precise pore dimensions and placement on the sidewalls of the polyhedron. The sidewall pore placement is mapped onto 2D panels (Figure 1 g–i) that are interconnected with hinges and used for self-folding of the polyhedron. Since the pores are patterned in two dimensions, it is possible to use extremely precise and well-developed patterning methods, such as photolithography, electron-beam lithography, and soft lithography. Our patterning technique also enables pore patterns designed by numerical simulations to be directly transferred to the computer-aided design (CAD) software

[*] Dr. Y. V. Kalinin, J. S. Randhawa, Prof. D. H. Gracias
Department of Chemical and Biomolecular Engineering
Johns Hopkins University
3400 North Charles Street, Baltimore, MD 21218 (USA)
Fax: (+1) 410-516-5510
E-mail: dgracias@jhu.edu
Homepage: http://www.jhu.edu/chembe/gracias/
Prof. D. H. Gracias
Department of Chemistry, Johns Hopkins University (USA)

[**] This research was supported by the NIH Director's New Innovator Award Program, part of the NIH Roadmap for Medical Research, through grant number 1-DP2-OD004346-01. Information about the NIH Roadmap can be found at http://nihroadmap.nih.gov. We thank Prof. Peter Devreotes, Elizabeth Cha, Kai-Wen Pai, Christina Randall, Rohan Fernandes, and Svetlana Ratner for valuable suggestions and discussions, and Prof. Mingming Wu and Kasyap Vasudevan for the RP437 strain of *E. coli*.

Supporting information for this article is available on the WWW under http://dx.doi.org/10.1002/anie.201007107.

used to generate the lithography masks. The fabrication approach is highly parallel, precise, and affords considerable versatility in the shape, size, density, and pattern of pores. Elsewhere, we have demonstrated that containers can be constructed with sizes ranging from 100 nm[18] to several millimeters, and with a variety of material compositions.[14,16] Hence, this versatility in fabrication coupled with our present approach could be used to generate chemical patterns on a range of size scales.

To enable diffusion-based chemical-pattern release, containers can be easily loaded by immersing them in the desired chemical, which diffuses into the container through the pores. The containers are also reusable (the containers can be washed out by immersion in solvents and then reused by immersion in the desired chemical), mobile, and mechanically robust, and can be manipulated with tweezers or pipettes without any breakage. Our surface-tension-based self-folding method also utilizes liquefying hinges at the periphery of the 2D panels. This approach results in robust sealing of the edges and corners of the polyhedral containers.[14] In contrast to porous polymer particles,[2,19–22] which soak up the chemical within a cross-linked matrix, our containers physically entrap the chemicals.[23] Hence, chemical encapsulation is less susceptible to chemical fouling and less dependent on the molecular properties of the chemical or details of the matrix-synthesis process. As a result, the containers can be used to generate patterns with a wide range of chemicals.

Experimentally, we lithographically patterned and self-assembled nickel-based containers. Subsequently, containers could be coated with gold to render them chemically and biologically inert[24,25] and to reduce the dimensions of the pores (by varying the thickness of the coating). Elsewhere, we showed that these containers can also be fabricated with alternative materials, such as biocompatible polymers.[16] At the present time, however, metallic containers offer the greatest precision in terms of pore definition and edge sealing, whereas the seamless edge sealing of polymeric containers is still challenging. Hence, we utilized metallic containers for this demonstration.

To quantify chemical-gradient formation, we loaded the containers by immersing them in an aqueous fluorescein solution. Fluorescein, a fluorescent water-soluble chemical with a low molecular weight, enabled us to visualize the pattern and also quantify its concentration by using fluorescence microscopy. After carefully rinsing the containers to remove excess fluorescein from their exterior, we positioned the containers in a stationary gel and observed that fluorescein was released from the containers. Numerical simulations and observations for the case of planar (2D) chemical patterns (such as linear gradients) were in excellent agreement with the experimental data (see the Supporting Information, including Figure S1, for complete details).

To generate 3D spatial patterns, we utilized two conceptually different strategies. In one strategy, the overall shape of the container was chosen to closely match the desired 3D spatial profile. For example, conical gradients were formed when chemicals were released from triangular-pyramid-shaped containers (Figure 2a–e), and experimentally observed gradients were in agreement with numerical simulations. The container-fabrication methodology can be used to assemble containers with alternative polyhedral shapes, such as triangular prisms with different lengths (Figure 2f), to enable these gradients to be generated over small or large length scales.

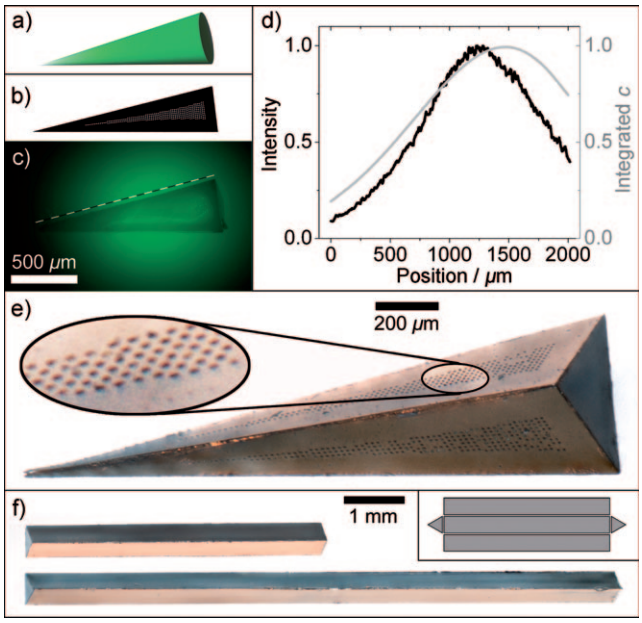

Figure 2. Generation of 3D spatial patterns by varying container shape. a) An idealized illustration of a conical gradient. b) Schematic diagram of a single triangular panel with pores enclosed in a wedge-shaped area that was found in numerical simulations to generate a linear gradient along its length. c) Fluorescence image showing the successful generation of the conical chemical gradient with a pyramid-shaped container with triangular faces patterned according to (b). d) Plot of the experimentally measured chemical concentration (thick black line) compared to that of the numerical calculation (thin gray line) along the dashed line shown in (c). e) Magnified optical image of the container used to generate the conical gradient pattern. f) Triangular-prism-shaped containers with two different lengths. The inset shows the 2D geometry of interconnected panels.

Our second strategy was to engineer the pattern of pores on one or many faces of the container. A combination of 2D lithographic patterning and self-folding enabled the container faces to be precisely patterned in all three dimensions. Moreover, this patterning can be carried out in an asymmetric manner. We describe an example of chemical release in the shape of a helix, which is a representative 3D space curve. Since a helix can be thought of as a curve wrapped around a cylinder, we utilized a parallelepiped-shaped container. One pattern of slits that was found in simulations to release chemicals in a helix is shown in Figure 3a. A container with this slit arrangement was fabricated and assembled (Figure 3b). Fluorescein was loaded into this container, and when the container was placed in a gel, a helical pattern (Figure 3c) was observed, the spatial profile of which was in good agreement with the simulations (Figure 3d). Thus, this strategy directs local pattern formation, whereas the previous strategy dictates the global boundaries of the pattern. Together, these two strategies enable the generation of 3D

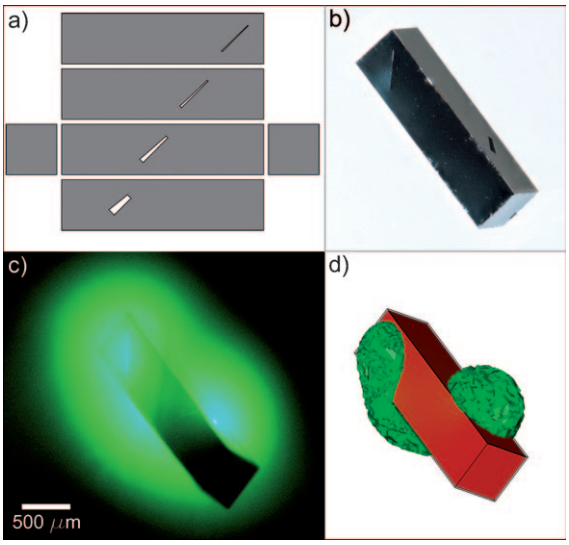

Figure 3. Generation of 3D spatial patterns by varying pore placement. a) CAD layout showing the 2D panel geometry and the patterned slits. b) Optical image of a container fabricated with the panel design shown in (a). In the assembled container, the slits line up along a helical path. c) Experimental result and d) numerical simulation of the helical spatial pattern of fluorescein.

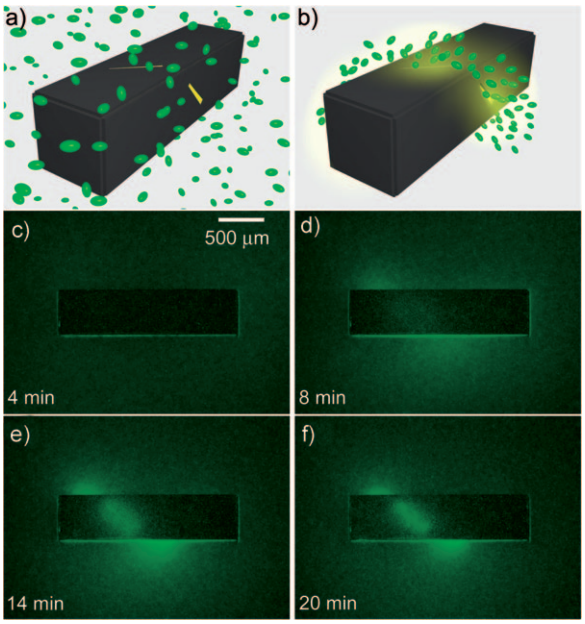

Figure 4. Direction of the chemotactic self-organization of *E. coli* in the shape of a helix. a,b) Conceptual representation of the desired chemotactic self-organization. At the start of the experiment, the chemoattractant is confined to the container, and the *E. coli* cells (represented by green ellipsoids) are distributed uniformly throughout the medium (a). The *E. coli* cells self-organize in a helical pattern based on the underlying chemical pattern once the chemoattractant (yellow) is allowed to diffuse out of the container (b). c–f) Experimental realization of the concept. Time-lapse images of green fluorescent *E. coli* as the bacteria self-organized in a helical pattern around a container with slits as shown in Figure 3. The time indicated at the bottom of each image is the time lapse after the container was placed in the medium containing *E. coli*. The underlying chemical pattern was not visualized in this experiment.

spatial patterns of virtually any shape consistent with the diffusion process in stationary media.

Our demonstrations provide convincing proof-of-concept that a variety of 3D patterns can be generated and sustained by the release of chemicals from a container. We anticipate that these containers can be utilized for the in vitro generation of chemical patterns that are of importance in cell and tissue functions, such as in microbial quorum sensing, organ and embryonic development, angiogenesis, and the workings of the immune system. To demonstrate the applicability of our concept to the in vitro organization of living systems in specific 3D geometries, we present a demonstration of chemotactic organization of bacteria in a well-defined geometric space curve. Our hypothesis was that chemotactic cells could be guided by a chemoattractant pattern generated by the container (Figure 4 a,b). *Escherichia coli* (*E. coli*) bacteria, which are well-characterized prokaryotes often used in chemotaxis studies, were chosen for the demonstration. We utilized the chemical-helix-generating container (Figure 3 b), which was loaded with L-serine, a known chemoattractant for *E. coli*.[26] The initial chemoattractant concentration inside the container, the shape of the container, and the slit geometry determined the spatiotemporal characteristics of the *E. coli* pattern (such as the time it would take *E. coli* to self-organize into a helix as well as cell-density variations in the resulting bacterial distribution[26]). The container was placed in a chamber filled with motility medium, and bacteria expressing green fluorescent protein (GFP) were seeded at a low density uniformly around the container. A series of time-lapse fluorescence images (Figure 4 c–f; see Video S1 in the Supporting Information) show a transition from a uniform bacterial distribution (Figure 4 c) to a helical bacterial distribution in the vicinity of the container (Figure 4 d–f). This study demonstrates the applicability of these chemical-pattern-generating containers for in vitro cell studies.

Other applications, such as studies involving mammalian cells, may necessitate the generation of 3D chemical patterns over longer time scales. The temporal stability of the chemical pattern depends on the duration of chemical release from the containers by diffusion. Analytical estimates (see the Supporting Information) show that the most straightforward way to alter the maximal duration of chemical release (τ) is by varying the ratio of the container size (d) to the total area of the pores (A): $\tau \approx (\pi/6)\,(d^3 w)/(A D)$. In this equation, w is the container wall thickness, and D is the diffusion coefficient, whose magnitude depends on the specific chemical and medium. If the container size d is increased to 1 mm and the total pore area is decreased to $A = 6 \times 10^4$ nm^2, the characteristic timescale τ of pattern formation in stationary media for a molecule with a diffusion constant of $D = 4.2 \times 10^{-10}$ m^{2}s^{-1} (which corresponds to that of fluorescein dye,[27] $w = 1$ μm) becomes approximately 2×10^9 s, that is, comparable to a human lifetime. Alternative methods can be used to speed up the loading of such containers (see the Supporting Information).

Numerical simulations corroborate and refine these estimates and enable quantitative temporal data sets to be plotted (Figure 5 a) for different combinations of container

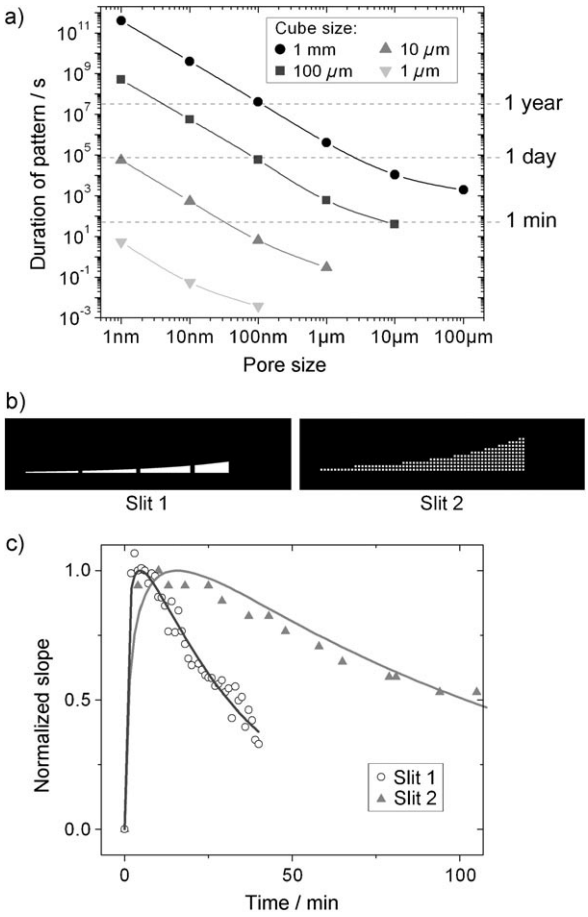

Figure 5. Numerical and experimental results showing temporal control over the chemical patterns. a) Calculated chemical-release times for cubic containers with varying cube and pore sizes for the release of a chemical with $D = 4.2 \times 10^{-10}$ m^2 s^{-1}. The data points plotted correspond to the period during which at least 90% of the maximal concentration is maintained at a distance d from the center of the container. b) Schematic illustration of two panels with slits that form a similar geometric pattern but with different individual pore sizes and porosity. c) Experimental data points and simulation data (solid lines) showing that duration for a linear spatial gradient is extended by roughly a factor of three for containers with slit 2 as compared to those with slit 1.

and pore size. The data sets are not restricted to chemicals with a diffusion coefficient similar to that of fluorescein. Since the diffusion coefficients of most chemicals scale with their molecular weight (M_w) according to the relationship $D \propto (M_w)^{-n}$, with $n \approx 0.5$ for water,[28] release times will be longer for molecules larger than fluorescein dye and shorter for smaller molecules. The temporal release characteristics are also affected by the pore distribution (see Figure S2 c,d in the Supporting Information).

Simulations also confirmed that the temporal characteristics can be readily varied while the same spatial release pattern is preserved. Experimentally, in two dimensions, the size of the pores on the panels is limited by the resolution of lithographic patterning. However, after the self-assembly of metallic containers, the size of pores can be uniformly decreased by Au electrodeposition (see Figure S3). The technique is not limited to isolated pores; pores that form complicated patterns can also be uniformly reduced in size. For example, the slit used to generate linear gradients (see Figure S1 a,b) was broken by CAD into individual similarly sized pores 12 μm in size (Figure 5 b; see also Figure 2 b,e), which were subsequently shrunk to about 2 μm by plating gold on the exterior of the assembled container; consequently, the porosity was also decreased. This process involving pixilation with subsequent gold electroplating preserved the linear shape of the generated chemical pattern but increased the time over which the gradient persisted by roughly a factor of three (Figure 5 c). Our experimental results confirm that by using smaller-sized pores within the same pattern on the container, one can retain the spatial characteristics of the chemical profile while increasing the time over which the pattern persists.

In summary, we have described an in vitro method that provides unprecedented precision and versatility in the generation of 3D chemical patterns in stationary media for a variety of applications in chemistry,[23] microbiology, cell signaling, and tissue development. In biological applications, patterns can function as chemical scaffolds for the study of important cellular functions in vitro. The 3D chemical release can also be used with single or multiple containers to engineer spatiotemporal characteristics of chemical reactions and hence enable 3D reaction-diffusion-based pattern formation. Our containers have relatively simple release kinetics typical of membrane-controlled reservoir systems. In our present demonstration, the containers were composed of nickel, a ferromagnetic metal, and coated with gold, an inert material. Owing to the inertness of gold, the containers can be used to encapsulate a range of chemicals. Additionally, we have previously demonstrated that the containers are nontoxic to mammalian cells[29] and hence appropriate for in vitro applications. The ferromagnetic composition enables the containers to be remotely steered by using magnetic fields and heated to alter chemical gradients[30,31] and thus provides a route for the generation of dynamical chemical patterns, if needed. Herein, we have demonstrated the generation of one space curve; however, we anticipate that chemicals could also be released in a variety of space curves by variation of the geometric design parameters.

Experimental Section

Numerical simulations: Numerical simulations were carried out with COMSOL Multiphysics (COMSOL, Inc.). Solutions of the time-dependent diffusion equation were sought in the geometry corresponding to the patterned container. The container was surrounded by a stationary medium with a volume approximately 100 times larger than that of the container. We assumed that the chemical concentration at the outer boundaries of the medium was maintained at zero at all times. The accuracy of the model was independently verified by numerical calculations on the diffusion coefficient of fluorescein from the experimental data shown in Figure 5 c. This value was found to be 4.2×10^{-10} m^2 s^{-1} and is in excellent agreement with reported data.[27]

Container fabrication: The patterns and slit shapes obtained in our numerical simulations were exported to AutoCAD (Autodesk, Inc.) and printed on masks at 40000 dpi. The masks were used for the fabrication of 2D panels and solder hinges according to the procedures reported previously.[14,23] The panels with hinges were

then released from the wafers and heated above the melting point of solder, at which point they spontaneously folded into 3D containers. The self-folding process was driven by a minimization of the surface energy of the molten hinges and is described in detail elsewhere.[14] The hinges were designed to completely seal the edges and the corners of the containers. Gold (Au) was coated on the inside and outside of the cubes by electrodeposition after assembly. The final size of the pores was determined by the duration and current density of electrodeposition.[25]

Chemical loading: All containers were loaded with the appropriate chemical by soaking them in aqueous solutions overnight. We utilized solutions of approximately 0.1, 7, and 1 mM of fluorescein, uranine (sodium salt of fluorescein, with a much higher solubility in water), and L-serine (in chemotaxis buffer), respectively.

Imaging and diffusion studies: Diffusion from fluorescein-filled containers was imaged by submerging the containers into either a 1 mm tall polydimethylsiloxane (PDMS) chamber or glass capillaries approximately 1–5 mm in diameter, which were filled with either 1 or 3% (w/v) agarose gel (to suppress convection and undesired flows). Previous studies have shown that the fluorescence intensity from fluorescein dyes depends linearly on the concentration of the dye.[26,32] The linearity of the camera was verified before any experiments were conducted.

Bacterial culturing and bacterial 3D pattern formation by chemotaxis: *E. coli* strain RP437 transformed with plasmid pTrc-GFP (a kind gift of M. DeLisa, Cornell University) was grown according to the protocol reported previously.[11,26] Cultures grown overnight were diluted 1:17 into fresh media, isopropyl β-D-1-thiogalactopyranoside (IPTG) was added to a final concentration of 1 mM (to induce the expression of fluorescent proteins), and bacteria were grown in a shaker bath for three more hours. Prior to experiments, cells were centrifuged for 2 min at 1500*g*, the supernatant was removed, and the dense cell pellet was resuspended in chemotaxis buffer (10 mL; 10 mM phosphate buffer–0.1 mM ethylenediaminetetraacetic acid–1 μM methionine–10 mM lactic acid (pH 7.3)) to the final optical density $OD_{600} \approx 0.05$.

To enable chemotactic organization, bacteria were injected into a rectangular PDMS chamber with dimensions 1 mm (height) by 7 mm (width) by 7 mm (depth). A helical-pattern-generating container measuring 2 mm × 500 μm × 500 μm (shown in Figure 3) was placed at the center of the chamber.

Received: November 11, 2010
Published online: February 17, 2011

Keywords: chemical patterning · chemotaxis · drug delivery · self-assembly · tissue engineering

[1] J. A. Burdick, G. Vunjak-Novakovic, *Tissue Eng. Part A* **2009**, *15*, 205.
[2] G. Mapili, Y. Lu, S. C. Chen, K. J. Roy, *J. Biomed. Mater. Res. Part B* **2005**, *75B*, 414.
[3] V. M. Weaver, O. W. Petersen, F. Wang, C. A. Larabell, P. Briand, C. Damsky, M. J. Bissell, *J. Cell Biol.* **1997**, *137*, 231.
[4] K. Wolf, I. Mazo, H. Leung, K. Engelke, U. H. von Andrian, E. I. Deryugina, A. Y. Strongin, E. B. Brocker, P. Friedl, *J. Cell Biol.* **2003**, *160*, 267.
[5] E. Cukierman, R. Pankov, D. R. Stevens, K. M. Yamada, *Science* **2001**, *294*, 1708.
[6] C. Fischbach, R. Chen, T. Matsumoto, T. Schmelzle, J. S. Brugge, P. J. Polverini, D. J. Mooney, *Nat. Methods* **2007**, *4*, 855.
[7] C. M. Nelson, M. M. VanDuijn, J. L. Inman, D. A. Fletcher, M. J. Bissell, *Science* **2006**, *314*, 298.
[8] N. L. Jeon, H. Baskaran, S. K. W. Dertinger, G. M. Whitesides, L. Van de Water, M. Toner, *Nat. Biotechnol.* **2002**, *20*, 826.
[9] V. V. Abhyankar, M. W. Toepke, C. L. Cortesio, M. A. Lokuta, A. Huttenlocher, D. J. Beebe, *Lab Chip* **2008**, *8*, 1507.
[10] B. Mosadegh, C. Huang, J. W. Park, H. S. Shin, B. G. Chung, S. K. Hwang, K. H. Lee, H. J. Kim, J. Brody, N. L. Jeon, *Langmuir* **2007**, *23*, 10910.
[11] Y. Kalinin, S. Neumann, V. Sourjik, M. Wu, *J. Bacteriol.* **2010**, *192*, 1796.
[12] S. Freiberg, X. X. Zhu, *Int. J. Pharm.* **2004**, *282*, 1.
[13] X. J. Zhao, S. Jain, H. B. Larman, S. Gonzalez, D. J. Irvine, *Biomaterials* **2005**, *26*, 5048.
[14] T. G. Leong, P. A. Lester, T. L. Koh, E. K. Call, D. H. Gracias, *Langmuir* **2007**, *23*, 8747.
[15] J. H. Cho, A. Azam, D. H. Gracias, *Langmuir* **2010**, *26*, 16534.
[16] A. Azam, K. E. Laflin, M. Jamal, R. Fernandes, D. H. Gracias, *Biomed. Microdevices*, DOI: 10.1007s10544-010-9470-x.
[17] D. J. Filipiak, A. Azam, T. G. Leong, D. H. Gracias, *J. Micromech. Microeng.* **2009**, *19*, 075012.
[18] J. H. Cho, D. H. Gracias, *Nano Lett.* **2009**, *9*, 4049.
[19] Y. Y. Yang, T. S. Chung, X. L. Bai, W. K. Chan, *Chem. Eng. Sci.* **2000**, *55*, 2223.
[20] R. P. Batycky, J. Hanes, R. Langer, D. A. Edwards, *J. Pharm. Sci.* **1997**, *86*, 1464.
[21] W. J. Rosoff, R. McAllister, M. A. Esrick, G. J. Goodhill, J. S. Urbach, *Biotechnol. Bioeng.* **2005**, *91*, 754.
[22] C. E. Semino, J. R. Merok, G. G. Crane, G. Panagiotakos, S. G. Zhang, *Differentiation* **2003**, *71*, 262.
[23] T. Leong, Z. Y. Gu, T. Koh, D. H. Gracias, *J. Am. Chem. Soc.* **2006**, *128*, 11336.
[24] C. L. Randall, A. Gillespie, S. Singh, T. G. Leong, D. H. Gracias, *Anal. Bioanal. Chem.* **2009**, *393*, 1217.
[25] C. L. Randall, T. G. Leong, N. Bassik, D. H. Gracias, *Adv. Drug Delivery Rev.* **2007**, *59*, 1547.
[26] Y. V. Kalinin, L. L. Jiang, Y. H. Tu, M. M. Wu, *Biophys. J.* **2009**, *96*, 2439.
[27] C. T. Culbertson, S. C. Jacobson, J. M. Ramsey, *Talanta* **2002**, *56*, 365.
[28] R. W. Baker, *Controlled Release of Biologically Active Agents*, Wiley, New York, **1987**.
[29] C. L. Randall, Y. V. Kalinin, M. Jamal, T. Manohar, D. H. Gracias, *Lab Chip* **2011**, *11*, 127.
[30] B. Gimi, D. Artemov, T. Leong, D. H. Gracias, Z. M. Bhujwalla, *Magn. Reson. Med.* **2007**, *58*, 1283.
[31] H. K. Ye, C. L. Randall, T. G. Leong, D. A. Slanac, E. K. Call, D. H. Gracias, *Angew. Chem.* **2007**, *119*, 5079; *Angew. Chem. Int. Ed.* **2007**, *46*, 4991.
[32] D. A. Walker, *J. Phys. E* **1987**, *20*, 217.

